TU Delft

Delft University of Technology

Document Version
Final published version

Licence
CC BY

Citation (APA)
Tavaststjerna, M. J., Connolly, R., Caliari, S., Picken, S. J., & Garcia, S. J. (2026). From patterned to continuous hydrophilic surface lubrication as strategies to obtain durable low ice adhesion coatings. *Progress in Organic Coatings*, *220*, Article 110435. https://doi.org/10.1016/j.porgcoat.2026.110435

Important note
To cite this publication, please use the final published version (if applicable).
Please check the document version above.

Copyright
In case the licence states “Dutch Copyright Act (Article 25fa)”, this publication was made available Green Open Access via the TU Delft Institutional Repository pursuant to Dutch Copyright Act (Article 25fa, the Taverne amendment). This provision does not affect copyright ownership.
Unless copyright is transferred by contract or statute, it remains with the copyright holder.

Sharing and reuse
Other than for strictly personal use, it is not permitted to download, forward or distribute the text or part of it, without the consent of the author(s) and/or copyright holder(s), unless the work is under an open content license such as Creative Commons.

Takedown policy
Please contact us and provide details if you believe this document breaches copyrights.
We will remove access to the work immediately and investigate your claim.

This work is downloaded from Delft University of Technology.

Progress in Organic Coatings 220 (2026) 110435

Contents lists available at ScienceDirect

Progress in Organic Coatings

journal homepage: www.elsevier.com/locate/porgcoat

From patterned to continuous hydrophilic surface lubrication as strategies to obtain durable low ice adhesion coatings

M.J. Tavaststjerna [a,*], R. Connolly [a], S. Caliari [a], S.J. Picken [b], S.J. Garcia [a]

[a] Department of Aerospace Structures and Materials, Faculty of Aerospace Engineering, Delft University of Technology, Kluyverweg 1, 2629, HS, Delft, the Netherlands
[b] Department of Chemical Engineering, Faculty of Applied Sciences, Delft University of Technology, Van der Maasweg 9, 2629, HZ, Delft, the Netherlands

ARTICLE INFO

Keywords:
Ice adhesion
Anti-icing
Molecular water layer
Aqueous lubricating layer
Non-freezable water
Quasi liquid layer (QLL)

ABSTRACT

In aviation, ice removal from surfaces primarily relies on energy-intensive active de-icing systems and anti-icing fluids with significant operational and environmental impact. Alternatively, passive low-icing or low-ice-adhesion surfaces may be used. However, existing passive anti-icing and low-ice adhering materials often lack durability, rely on complex fabrication methods, or cannot be integrated into certified coating systems. Similar challenges are faced in other fields such as communications, ships, and cryogenic preservation. In this work, we introduce and compare several scalable PFAS-free surface-modification strategies based on surface lubrication to obtain low ice adhesion. A robust home-made multichannel ice adhesion testing device was further developed and used across the study. The strategies, applied to three polymeric substrates (a commercial aircraft polyurethane (PU) topcoat, polyvinyl chloride (PVC), and polypropylene (PP)), were: (i) controlled UV exposure, (ii) silicone-oil microdroplet contamination, (iii) hydrophilic micropatterns based on covalently grafted Poly(2-hydroxyethyl methacrylate) (PHEMA), and (iv) a UV-curable hydrophilic spray coating based on 2-(Methacryloyloxy)ethyltrimethylammonium chloride (DMC). UV degradation showed a minor yet measurable effect on the reduction of ice adhesion. On the other hand, surfaces coated with molecular water layer-forming treatments (PHEMA patterns and DMC) significantly lowered ice adhesion at −10 °C, outperforming oil microdroplets. Together with homogeneous PHEMA-grafts, the DMC coating achieved the lowest adhesion strengths—consistently below 20 kPa in cyclic testing—attributed to the formation of a non-freezing surface water layer. These results demonstrate that PFAS-free water-lubricating hydrophilic coatings offer a promising pathway toward a new generation of effective passive anti-icing materials.

1. Introduction

Ice accretion and frost formation on surfaces present persistent safety and operational challenges across numerous sectors, including energy production [1,2], telecommunications [3,4], transportation [5], and refrigeration [6]. Among these, the aviation industry is particularly vulnerable due to the severe consequences that even small amounts of ice can impose on aerodynamic performance [7–11]. Ice buildup on aircraft wings, propellers, and sensors alters airfoil geometry, increases drag, reduces lift, and increases the aircraft's weight, ultimately compromising both efficiency and safety. Because aircraft routinely operate in mixed-phase clouds, freezing rain, and cold and humid atmospheres, any surface exposed to the airflow becomes susceptible to repeated icing events. As global air traffic continues to expand, mitigating icing risks efficiently and sustainably has become an increasingly important engineering challenge.

Commercial aircraft currently rely almost exclusively on active anti-icing systems, the most common being electro-thermal heating. [12,13] Embedded heating elements supply continuous or cyclic thermal energy to maintain surface temperatures above freezing. Although effective and reliable, such systems impose considerable penalties in terms of energy consumption, fuel use, and maintenance requirements. For modern passenger aircraft, thermal anti-icing can account for several percent of overall fuel requirements, corresponding to increased carbon emissions and operational costs. Furthermore, adding heaters and power lines increases both structural complexity and aircraft weight. These limitations have motivated a growing interest in passive anti-icing materials, which aim to prevent or mitigate icing without requiring external energy input. [14–16]

One promising passive strategy is the development of surface

* Corresponding author.
E-mail address: m.j.tavaststjerna@tudelft.nl (M.J. Tavaststjerna).

https://doi.org/10.1016/j.porgcoat.2026.110435
Received 7 May 2026; Received in revised form 20 June 2026; Accepted 7 July 2026
Available online 17 July 2026
0300-9440/© 2026 The Authors. Published by Elsevier B.V. This is an open access article under the CC BY license (http://creativecommons.org/licenses/by/4.0/).

coatings with ultra-low ice adhesion strength. [15,17] If the adhesion between ice and the aircraft coating is sufficiently small—typically specified to be under <30 kPa—then ice could be removed continuously by wind flow (12 m/s) around the airfoil during flight, hence preventing dangerous ice accumulation without the need for heating or chemical de-icing. [16,18,19] Although numerous materials and surface treatments with low ice adhesion have been reported in the literature, none have yet reached commercial implementation on aircraft. Coatings with promising laboratory performance often fail due to issues with scalability, durability, surface contaminations, and/or complex fabrication routes. From an industrial standpoint, an ideal passive anti-icing solution should be inexpensive, fast to apply, compatible with existing aerospace coatings, and mechanically robust under UV exposure, abrasion, dust contamination, and chemical stressors.

To design such coatings, it is essential to consider how ice adhesion can be minimized. Several strategies have been explored extensively: hydrophobic and superhydrophobic coatings, soft elastic substrates, and oil-infused polymers (also referred to as liquid-infused surfaces). Each approach can reduce ice adhesion through a different mechanism, but each also introduces limitations for long-term aircraft use. [20] Superhydrophobic materials utilize structured and nano-fabricated surface topologies to reduce ice adhesion by minimizing ice-substrate contact area. [21] However, superhydrophobic surfaces typically depend on delicate micro- or nano-textured topographies that are susceptible to abrasion and contamination. [22] Moreover, under humid or icing conditions, liquid penetration into the nano-features can also drastically increase ice adhesion due to mechanical interlocking. [23,24] Elastic PDMS-based surfaces [25], which deform at the ice–substrate interface, can also lower adhesion by dissipating shear stresses during detachment; however, their inherent softness makes them vulnerable to mechanical damage and abrasion. Oil-infused polymers [26,27] create an effective lubricating oil film between the ice and the solid substrate, but the infused oils (typically silicone, perfluoropolyether (PFPE), or mineral oils) tend to deplete over time, leading to increased ice adhesion [28]. In all these strategies, durability remains the biggest limiting factor for industrial applications.

An emerging alternative approach relies on the formation of a stable aqueous lubricating layer at the ice–substrate interface [18,19,29,30,32–35]. This strategy is particularly attractive because it can provide low interfacial shear strength without relying on fragile surface roughness, soft bulk elasticity, or externally supplied oils. This concept is also described in the literature using terms such as quasi-liquid layer (QLL), non-freezing water layer, or liquid-like molecular water layer (MWL). Such layers arise when water molecules form strong interactions with certain chemical groups at the surface, preventing them from crystallizing at typical freezing temperatures. [36–38] On a molecular level, this behaviour is typically attributed to strong hydrogen-bonding interactions with charged or hydrophilic groups that inhibit the cooperative rearrangement of water molecules required for ice nucleation. These non-freezing water layers function as atmospheric self-replenishing lubricants, dramatically reducing interfacial shear strength. Several studies [29,30,32], using this principle applied on hydrogels, polyelectrolyte networks, and PEG-modified elastomers, have reported ice adhesion strengths well below 30 kPa— which is considered low enough for passive aircraft anti-icing. However, most such materials lack the mechanical robustness, environmental resistance, or application simplicity required in aviation and other fields. The development of aqueous lubricating surfaces made from durable and scalable coating chemistries appears as an interesting development with potential for implementation in critical application domains.

While material innovation is a key challenge, a parallel issue complicates progress in the field of passive anti-icing coatings: a lack of standardized ice adhesion testing. [39] Ice adhesion is most commonly measured using a shear force-based push test, but different laboratories employ widely varying apparatus designs, loading geometries, ice formation protocols, pushing speeds, pushing heights, and temperature–humidity conditions. Recently, several studies have demonstrated that parameters such as actuator pushing speed and pushing height can significantly influence the measured adhesion strength. Yet most published reports do not fully disclose these parameters, making comparison of results difficult. The absence of standardization has led to large discrepancies in reported adhesion values for inherently similar materials, obscuring which anti-icing strategies are genuinely most effective, hence highlighting the need to properly report and compare surfaces under well-controlled testing and environmental conditions.

In this study, we address both the materials challenge and the testing challenge in the development of low-ice adhesion coatings. First, we designed a horizontal shear (push) test setup with accurate temperature and humidity control and multiple sample holders, thereby significantly increasing experimental output speed relative to conventional single-sample designs. This system enables more reproducible, transparent, and systematic testing of ice adhesion under well-defined conditions. Second, we evaluated several surface modification strategies on three polymeric substrates of practical relevance: a commercial aircraft polyurethane (PU) topcoat, poly(vinyl chloride) (PVC), and polypropylene (PP). The selected surface modifications aimed at studying and comparing the impact on ice adhesion of hydrophobic and hydrophilic continuous and patterned surface lubrication, and the impact of UV exposure on the surface ice adhesion properties. To this aim, selected polymers were treated in different manners: (i) exposed to UV light, simulating UV environmental degradation; (ii) covered with silicone oil droplets, mimicking potential maintenance-related contamination; (iii) surface modified with hydrophilic micropatterns, following our recent findings showing their potential to control frost nucleation and propagation [40] as well as ice nucleation during supercooled droplet impact [41]; and (iv) coated with a new UV-curable hydrophilic (2-methacryloyloxyethyl) trimethyl ammonium chloride (DMC)-based spray coating, designed to create a durable, charged surface capable of supporting the formation of a stable non-freezing water layer.

Together, these experiments in very well-controlled testing and environmental conditions aim to provide new insight into how aqueous lubricating layers, surface chemistry, and environmental exposures affect ice adhesion to polymeric materials and demonstrate the potential of aqueous lubricating, scalable, PFAS-free, durable, and energy-efficient passive anti-icing strategies for future aircraft technologies.

2. Experimental

2.1. Materials

The polyurethane coating evaluated in this study is a commercial topcoat currently used in aviation. While the product identity and formulation details are proprietary and therefore undisclosed, its widespread use ensures that the findings are directly applicable to real-world scenarios. The polyurethane was received as part of the full coating system on an AA2024-T3 metallic panel (surface treatment-epoxy primer-polyurethane). The PP and PVC (20 × 20 × 2 mm) polymeric substrates used in this work were purchased from S-Polytec GmbH. Glycidyl methacrylate (GMA, 97%), 2-hydroxyethyl methacrylate (HEMA, 97%), hydrophilic (2-methacryloyloxyethyl) trimethyl ammonium chloride (DMC, 75 wt% in H_2O), 4-cyano-4-(phenylcarbonothioylthio)pentanoic acid (CTA), 2,2′-azobis(isobutyronitrile) (AIBN, 98%), sodium azide (NaN3, 99.5%), triethylamine (TEA, 99.7%), copper (*I*)bromide (CuBr, 98%), copper(II) bromide (CuBr2, 99%), 2-bromoisobutyrylbromide (BIBB, 98%), trimethylolpropane triacrylate (TMPTA, technical grade) and the silicone oil were purchased from Merck Sigma. 2-Hydroxy-2-methylpropiophenone (Darocur 1173, >96%) was purchased from TCI Europe.

2.2. Preparation of samples exposed to UV

All substrates (PU, PP, and PVC) were exposed to a UV-A lamp (OmniCure S2000 UV Curing System, 320–500 nm) with an irradiance of 30 W/cm^2 for 5 h and 10 h. This treatment exposes the substrates to an irradiance 3000 to 30,000 times higher than that of natural sunlight (0.001–0.01 W/cm^2) and can be considered an accelerated degradation test simulant of UV aging.

2.3. Preparation of samples with hydrophobic oil droplets

All substrates (PU, PP, PVC) were coated with eight 1 μL-sized discrete droplets of silicone oil (an aircraft contaminant) using a calibrated micropipette. The droplets were manually distributed within the region of the substrate later exposed to the ice column in ice adhesion testing.

2.4. Preparation of PHEMA-coated surfaces

PU, PP, and PVC were homogeneously coated or stripped-pattern coated with poly(2-hydroxyethyl methacrylate) (PHEMA) via surface-initiated atom transfer radical polymerization (SI-ATRP) as reported elsewhere. [40] The stripe dimensions were selected based on our previous works on frost propagation and frozen droplet impact. [40,41] Briefly, to create the stripes, the substrates were first spin-coated with a bifunctional macroinitiator (PAzBrMA). Since the macroinitiator can be covalently attached to the surface via UV exposure, a UV mask with a constant stripe width of 150 μm and a stripe distance of 1.2 mm was used to fix the macroinitiator only at stripe locations upon exposure to a UV lamp (OmniCure S2000 UV Curing System, 320–500 nm) with 30 W/cm^2 for 5 min. This was followed by (i) rinsing to remove the unreacted PAzBrMA, (ii) a SI-ATRP of the hydrophilic 2-hydroxyethyl methacrylate (HEMA) monomer from the macroinitiator at the stripe locations, and (iii) rinsing again to remove the excess HEMA. The resulting samples are polymeric substrates (PU, PP, or PVC) patterned with hydrophilic polymer brushes (PHEMA), which are covalently anchored to the substrate surface. Samples uniformly coated with PHEMA were fabricated using the same protocol, omitting the patterned mask during the UV-exposure step.

2.5. Preparation of DMC-coated surfaces

To evaluate the concept of water-enriched cationic surfaces on ice adhesion, a UV coating using hydrophilic (2-methacryloyloxyethyl) trimethyl ammonium chloride (DMC) was designed. The hydrophilic DMC-coating formulation was prepared by mixing DMC (4 g, monomer), Darocur 1173 (0.16 g, type I photoinitiator), and TMPTA (2.88 g, cross-linker) in EtOH (20 g, solvent). The mixture was applied to the polymeric substrates using a spray gun with a nozzle diameter of 1.4 mm, followed by UV exposure (OmniCure S2000 UV Curing System, 320–500 nm) at 30 W/cm^2 for 15 min.

2.6. Water contact angle measurements

Water contact angle (WCA) measurements of the bare, UV-exposed, PHEMA-grafted, and DMC-coated polymer surfaces were performed using an optical contact angle goniometer (KSV CAM 200). Silicone-oil-contaminated samples are excluded from WCA measurements, as the liquid oil phase exhibits an intrinsically high-water repellency. Static contact angles were determined using the sessile drop (10 μL) method. Each measurement was repeated three times per sample. All contact angle measurements were conducted at an ambient temperature of 21 ± 2 °C and a relative humidity of 40 ± 5%.

2.7. Surface characterization

Laser scanning confocal microscopy (LSCM, Keyence VK-X1000) was used to obtain the areal surface roughness (Sa) using a 20× magnification lens for all samples except for the oil-contaminated surfaces. Silicone-oil-contaminated samples are excluded from roughness characterization, as the liquid oil phase exhibits an effectively zero surface roughness. LSCM was also used to determine the thickness of the PHEMA stripes and DMC coating via line profile analysis. For PHEMA-patterned samples, profiles were taken across individual stripes to measure the height difference between grafted and unmodified regions. For the DMC coating, a step edge was created by masking the substrate with adhesive tape prior to spray coating. After UV curing and tape removal, the coating thickness was obtained from the height difference across the step edge. The PHEMA-graft and DMC coating thicknesses were measured to be approximately 0.2 μm and 50 μm, respectively. Micro–FTIR (μ-FTIR, PerkinElmer Spotlight 400) was employed specifically to analyse the chemically micropatterned PHEMA-grafted surfaces. In addition, the effect of UV exposure on the chemical composition of PU, PVC, and PP substrates was investigated using an FTIR spectrometer (Spectrum 100, PerkinElmer). Spectra were collected in the range of 4000–600 cm^{-1}, with each spectrum obtained by averaging 32 scans.

2.8. Ice adhesion tests

The ice adhesion strength of the samples was measured using a custom-built horizontal push-off test setup (Fig. 1). The setup consists of a temperature- and humidity-controlled environmental chamber, an external circulating cooling unit (LAUDA ECO RE1050), a humidity control system, a set of five sample holders, and a linear actuator (LTA-HL with CONEX-CC controller) equipped with a calibrated load cell that can be displaced to the selected sample holder for multiple measurements under comparable environmental conditions. The chamber humidity was maintained below 10% relative humidity (5 ± 3%) using a low nitrogen flow to prevent unwanted frost formation. Prior to ice generation, the substrates were cooled to −10 ± 1 °C. Deionized water (RT) was then injected into a Teflon mould positioned on top of each cooled substrate sample to form cylindrical ice pillars with a diameter of 8 mm and a height of 8 mm. The water pillars were then allowed to freeze for approximately 30 min. Ice adhesion was measured by advancing the actuator at a constant speed of 0.01 mm/s, with the pushing tip positioned 2 mm above the substrate surface. This height was selected based on a previous validation study performed using a similar test setup, where operation at a pushing height of 2 mm was shown to provide reproducible measurements within the quasi-static regime. [42] The applied force was recorded as a voltage–time curve, from which the peak force required to detach the ice was extracted with the help of a calibration force-voltage calibration curve. The load cell was calibrated over a force range of 0.5–200 N. Although lower force signals could be detected, uncertainties in calibration linearity and repeatability at very low loads resulted in a practical detection limit of ~5 kPa. The ice adhesion strength was calculated by dividing this peak force by the ice–substrate contact area (Eq. 1). Each surface condition was tested at least five times.

$$\tau_{ave} = \frac{F}{A} = \frac{g \times V_{peak}}{A} = \frac{9,80665 \frac{m}{s^2} \times V_{peak}}{0.0503\ cm^2} \quad (1)$$

3. Results and discussion

3.1. Design, construction, and validation of the ice adhesion test setup

Ice-adhesion measurements reported in the literature comprise a wide range of experimental configurations, including centrifugal tests, vertical shear setups, and various custom-built horizontal push or pull

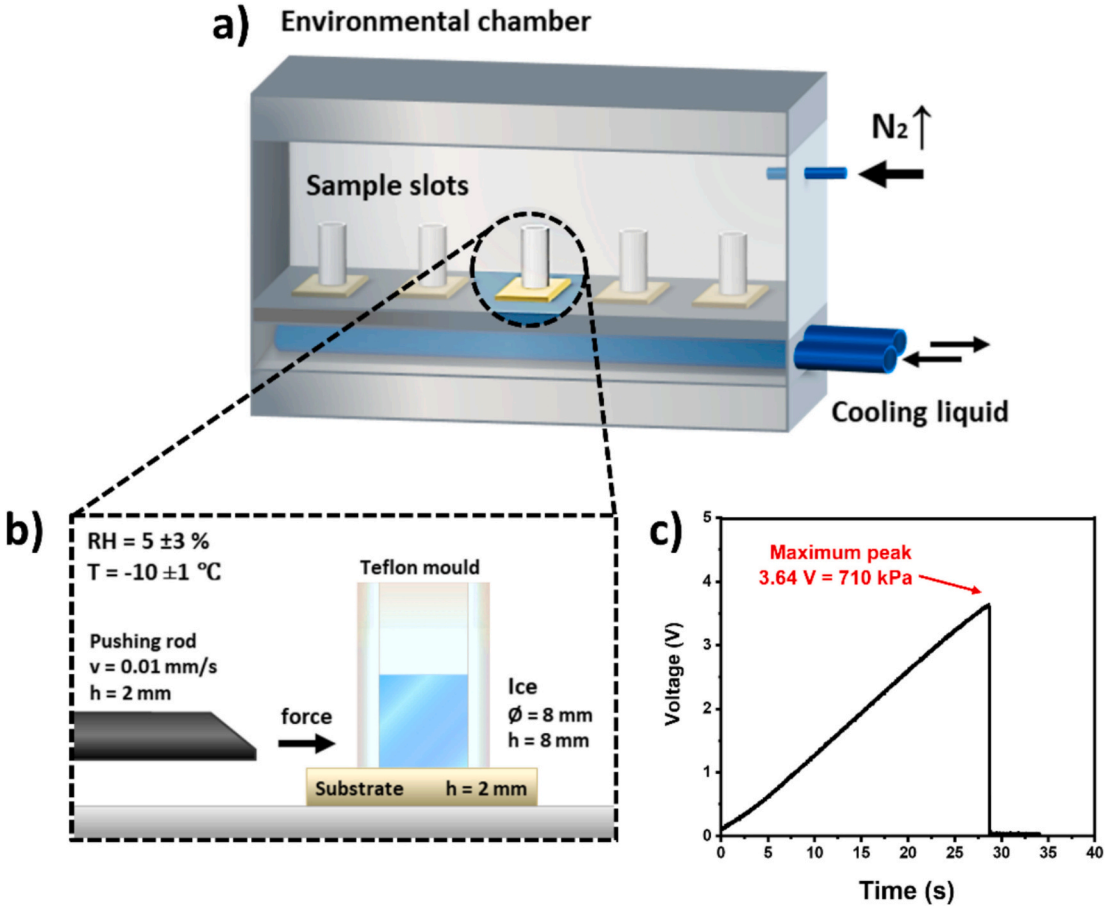


Fig. 1. Schematic representation of the ice adhesion experimental setup: (a) the environmental chamber with 5 sample holders, (b) the environmental and experimental parameters used in the push test in this work, and (c) an example of a voltage-time curve, which shows the peak voltage value at ice detachment and the corresponding ice adhesion strength derived from a voltage-force curve.

-test rigs. [39] This diversity complicates direct comparison between studies, particularly because the ice failure mechanism, environmental conditions, and mechanical test parameters strongly influence the measured ice adhesion strength. To ensure comparability with the majority of reported results, we designed and constructed a horizontal shear test (push test) setup, which remains the most widely used testing configuration in the literature.

Although conceptually straightforward, the push test is sensitive to several critical parameters that can dramatically affect the measured adhesion strength. Previous studies have demonstrated that pushing height, pushing speed, and testing temperature can shift the measured adhesion strength values by tens of kilopascals. [42–44] Based on these insights, our setup was designed to operate in a quasi-static regime, with the pushing height fixed at 2 mm and the pushing speed at 0.01 mm/s (out of a potential range of 0.01–1 mm/s). The selected pushing height was adopted from a previous validation study conducted using a similar test apparatus, where the influence of pushing height, speed, and ice diameter on the measured adhesion strength was systematically assessed. [42] Although lower pushing heights can reduce bending contributions within the ice pillar, a height of 2 mm was found to provide stable and reproducible measurements while allowing consistent testing of substrates with different thicknesses. These settings minimize dynamic or inertial contributions, ensuring that fracture occurs in a controlled manner dominated by interfacial failure.

A second major design goal was to obtain strict control of environmental testing conditions (humidity and temperature). The final setup (illustrated in Fig. 1) consists of a fully enclosed environmental chamber with independent control of temperature and humidity. The temperature inside the chamber and on the sample surfaces is regulated via a cooling-fluid channel beneath the sample holder plate, enabling cooling down to −50 °C. Humidity during the experiments is controlled by introducing a flow of inert nitrogen gas into the chamber, thus maintaining a constant 5 ± 3% relative humidity and preventing unwanted frost formation during testing. For real-time monitoring of both temperature and humidity, the chamber is also equipped with thermometers and manometers placed over the samples during testing. Furthermore, the test chamber was carefully vacuumed before each experiment to maintain clean, dust-free conditions.

Instead of testing only one sample per cooling cycle, the ice adhesion setup was equipped with a multi-sample platform featuring five sample positions arranged in a horizontal row. This design reduces experiment times, improves reproducibility, and facilitates the collection of statistically meaningful data. An alignment block placed above the sample holders ensures that all ice moulds are positioned consistently into the same locations between experiments. The alignment block also contains dedicated openings to fill the moulds with deionized water without disturbing the humidity balance inside the chamber.

During testing, the linear actuator—mounted on a horizontal guide rail in front of the chamber—is horizontally aligned with each sample using a manual positioning system. In a standard experiment, the pushing height is set to 2 mm and can be adjusted according to the thickness of the sample substrate. The actuator is equipped with a calibrated load cell and connected to a Picoscope data acquisition system with signal amplification and the Conex controller unit. To push the ice mould off the sample, the actuator is moved using the controller unit while the voltage and time are recorded via the Picoscope software.

To validate the reliability of the ice adhesion test setup, adhesion measurements were performed at −10 °C on several commonly used polymeric reference materials, including polytetrafluoroethylene (PTFE/Teflon), polyethylene (PE), polypropylene (PP), and polycarbonate (PC). A direct and systematic comparison with literature values for such substrates is challenging, as most published ice adhesion studies primarily focus on newly developed icephobic coatings and typically report only limited reference data. In addition, literature values are obtained using a variety of ice adhesion test configurations, including centrifugal, shear, and cone-based tests, which can further contribute to variability in reported adhesion strengths. Despite these limitations, the ice adhesion values obtained in this work (Fig. 2) fall within the ranges reported in the literature [45–49], with Teflon and PC showing the closest agreement with previously published values (~150 kPa and ~ 350 kPa, respectively). The measured adhesion strength for PE is slightly higher (~450 kPa vs. ~350 kPa), while that of PP is slightly lower than literature values (~150 kPa vs. ~300 kPa), which may be attributed to differences in surface roughness and chemistry (due to additives and molecular weight and composition variability), or the specific ice adhesion test configuration employed (e.g. RH, temperature). As detailed surface and material characteristics are rarely specified alongside ice adhesion results, the exact origin of these deviations cannot be conclusively determined. Overall, the close agreement between our measurements and data available in the literature, combined with the relatively low standard deviations found in our tests despite repeating the tests on different days, confirms the robustness and reliability of the experimental setup. This validation provides a solid and transparent foundation for the quantitative evaluation of the surface modifications presented in the following sections.

3.2. Sample preparation and surface characterization

Three substrate materials were selected for this work: a commercial aircraft polyurethane (PU) topcoat, polyvinyl chloride (PVC), and polypropylene (PP). The PU coating provides a direct connection to aviation applications, while PVC and PP serve as model engineering polymers widely used in industrial, medical, and infrastructure applications. These substrates differ substantially in their chemical compositions and surface chemistries, providing a meaningful framework for evaluating various anti-icing strategies.

Each substrate was modified using four different surface treatment strategies (schematically illustrated in Fig. 3): UV exposure for 5 h and 10 h (Fig. 3a), surface coverage with silicone oil microdroplets (Fig. 3b), micropatterns and uniform coverage by with covalently bonded hydrophilic PHEMA-brushes (Fig. 3c-i and 3c-ii), and a coating with a hydrophilic spray-coated UV-curable DMC topcoat (Fig. 3d).

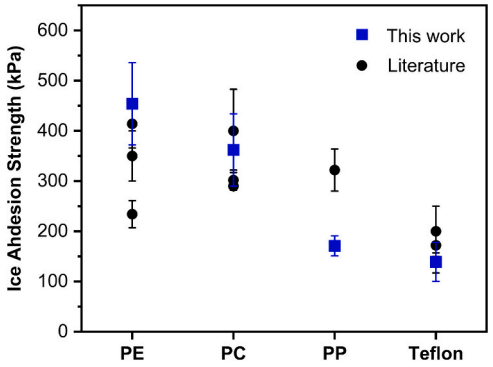


Fig. 2. Validation of the ice adhesion test setup by comparing ice adhesion strength values of common polymeric substrates measured in this work (blue squares) with literature values [45–49] (black circles) obtained using various ice adhesion test methods at temperatures of −10 ± 2 °C. (For interpretation of the references to colour in this figure legend, the reader is referred to the web version of this article.)

Micropatterning was achieved using a surface-initiated atom transfer radical polymerization (SI-ATRP) protocol as described in our previous publications. [40,41] First, a multifunctional macroinitiator (PAzBrMA) containing azide and bromide groups was covalently attached to the polymer surface through UV-induced C—N formation. The bromide moiety then served as the ATRP initiator for the polymerization of hydrophilic 2-hydroxyethyl methacrylate (HEMA), forming surface-grafted PHEMA chains. A patterned UV mask was used in the first step to restrict macroinitiator attachment to micrometer-scale striped regions (~150 μm width), resulting in local hydrophilic areas on the hydrophobic polymeric substrates. Without the UV mask, the samples were uniformly covered with the hydrophilic PHEMA brushes.

The (2-methacryloyloxyethyl) trimethyl ammonium chloride (DMC) based hydrophilic coating was prepared by spraying the coating formulation onto the substrate, followed by 15 min of UV curing. This process yields a hydrophilic, crosslinked coating with charged groups capable of forming strong hydrogen bonds with water molecules. Compared to micropatterning, this approach is faster, simpler, more scalable, and better suited for coating large, complex geometries such as aircraft surfaces.

The static water contact angle and confocal microscopy surface roughness of the studied samples can be seen in Fig. 4. The results show that UV exposure induces distinct, polymer-dependent changes in surface properties. Both PU and PVC exhibited a gradual decrease in water contact angle and surface roughness (Sa) with increasing UV exposure time (i.e., more hydrophilic and smooth surfaces). The static water contact angle of PU reduced from 87° to 74° after 10 h UV exposure, while the surface roughness reduced from 0.25 μm to 0.21 μm. For PVC, the corresponding transitions were from 96° to 92° in water contact angle and from 0.8 μm to 0.5 μm in surface roughness. The enhanced hydrophilicity is attributed to UV-induced chemical modifications[49], including dechlorination in PVC and the formation of polar, oxidized surface functionalities such as carbonyl and hydroxyl groups in PU. The incorporation of these chemical groups on PVC and PU surfaces is evident in the FTIR data (see Fig. 5), showing increasing transmittance peaks for OH stretch at ~3400 cm^{-1} and C═O stretch at ~1700 cm^{-1}. The concurrent reduction in surface roughness is likely associated with a UV-induced planarization effect at the outermost surface layers, resulting from photodegradation as reported elsewhere [50].

A different trend was observed for PP. While a slight planarization effect was also apparent (from 0.16 μm to 0.13 μm), PP showed a measurable increase in wettability at 5 h of UV exposure (from 101° to 87°), followed by a pronounced decrease in water wettability at 10 h UV exposure (contact angle increase up to 108°). This behaviour suggests the presence of competing processes: initial surface oxidation introduces hydrophilic functional groups that increase wetting, whereas prolonged UV exposure promotes degradation and hydrophobic recovery. This behaviour has been reported for polyethylene (LDPE) and poly(propylene) (PP) exposed to prolonged UV/VUV radiation (100–400 nm). [51] During this recovery process, UV-generated polar groups undergo bond scission and cross-linking, leading to the loss of surface oxidation products and the restoration of hydrophobic surface characteristics. This phenomenon is supported by the FTIR data in Fig. 5, showing subtle emerging C═O stretching peaks at ~1700 cm^{-1} on the PP surface after the initial 5 h of UV exposure, which later disappear after 10 h of exposure.

The surfaces modified with a continuous PHEMA grafted hydrophilic layer exhibited the lowest water contact angles among all investigated samples (WCA = 40 ± 3°). Since the reported wettability and roughness values correspond to fully grafted PHEMA regions, these reflect the intrinsic hydrophilicity of the grafted polymer stripes in PHEMA patterned surfaces. The grafting with PHEMA did not lead to a significant increase in surface roughness on any of the polymeric substrates, which is consistent with the relatively short PHEMA chain lengths obtained after 4 h of polymerization (< 0.3 μm) and our earliest reports on

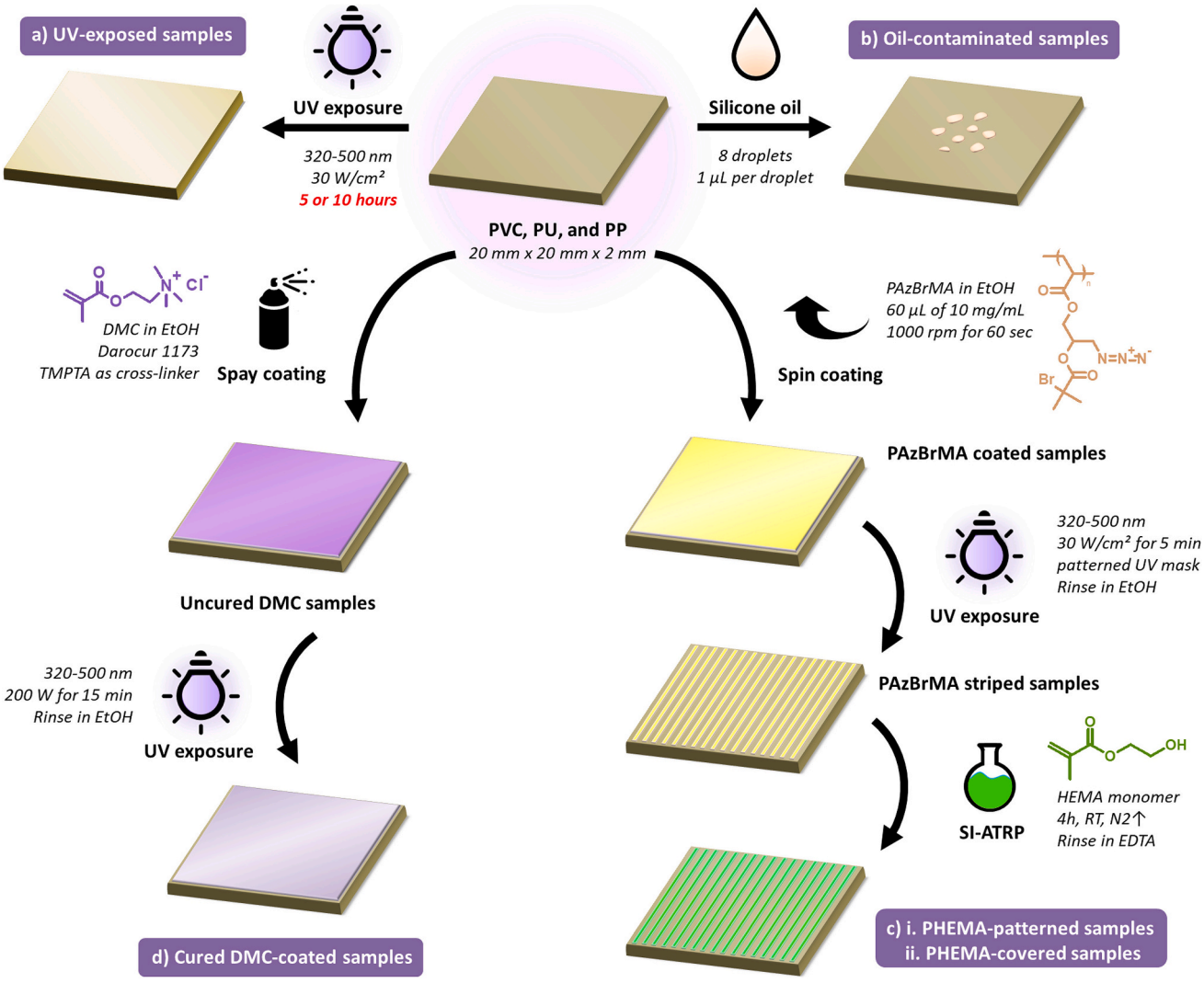


Fig. 3. Schematic overview of the surface modification strategies applied to the polymeric substrates (PVC, PU, and PP) investigated in this work: (a) UV exposure for 5 or 10 h, (b) contamination with silicone oil microdroplets, (c) hydrophilic grafting via surface-initiated ATRP of HEMA, and (d) spray application of a UV-curable hydrophilic DMC coating.

patterned surfaces. [40]

As intended, DMC-coated samples displayed low water contact angles and smooth surface topographies (WCA = 62 ± 1° and Sa = 0.25 ± 0.02 µm), independent of the underlying polymer substrate. This behaviour is consistent with the formation of a continuous, uniform, hydrophilic coating layer that effectively masks the substrate-specific surface properties.

Overall, these results demonstrate that the applied surface modification strategies induce controlled and polymer-specific changes in surface chemistry and morphology. As both wettability and surface roughness play key roles in governing water–surface interactions, these characteristics provide essential context for interpreting the ice adhesion behaviour discussed in the subsequent sections.

3.3. *Influence of UV exposure on ice adhesion*

The ice adhesion results for all investigated surfaces are summarized in Fig. 6. All measurements were conducted at −10 ± 1 °C and 5 ± 3% relative humidity, with at least five independent measurements taken per sample type. A representative force–displacement curve (recorded as voltage–time) is shown in Fig. 1, where the maximum voltage (V_{peak}) corresponds to the moment of ice detachment.

Among the unmodified substrates, the commercial PU topcoat exhibited the highest ice adhesion strength (824 kPa), reaching values comparable to or even exceeding values commonly reported for bare aluminium alloys (~600–1000 kPa). In contrast, PP showed the lowest ice adhesion (171 kPa), while PVC displayed intermediate behaviour (687 kPa). The poor performance of PU is particularly notable given its widespread use in aviation coatings, reinforcing the need for improved passive low ice adhesion coating solutions.

UV exposure revealed a clear divergence in ice adhesion behaviour, with PU and PVC responding differently from PP. For both PU and PVC, no-effect to a slight-increase in ice adhesion strength was observed with increasing UV exposure time, reaching 873 kPa (from 833 kPa) and 691 kPa (from 687 kPa) after 10 h, respectively. These minimal changes coincide with the measurable increased surface hydrophilicity observed in WCA measurements and the formation of oxidized surface functionalities confirmed by FTIR analysis (Fig. 5). It is hypothesized that the introduction of polar groups on a rigid surface enhances hydrogen bonding at the ice–surface interface, thereby promoting stronger adhesion. At the same time, UV-induced surface planarization [50] led to a reduction in surface roughness for both materials, which may partially counteract the effect of increased wettability. This balance between chemical and topographical changes, together with the known chemical resistance of PU and PVC to UV degradation, likely explains why the overall increase in ice adhesion is relatively small, particularly for PVC,

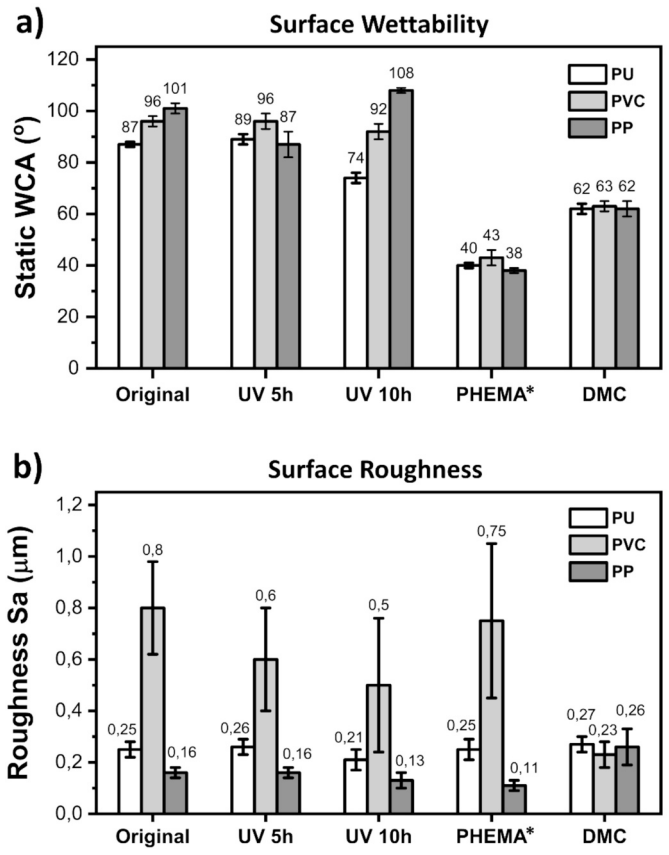


Fig. 4. Characteristic surface parameters showing: (a) Static water contact angles (WCA) and (b) Surface roughness values (Sa) of PU, PVC, and PP substrates in their original state and after UV exposure (5 h and 10 h), hydrophilic PHEMA grafting, and DMC coating. *Note 1*: Silicone-oil-contaminated samples are excluded, as the liquid oil phase exhibits an effectively zero surface roughness and intrinsically high-water repellency. *Note 2:* The values reported for PHEMA correspond to surfaces homogeneously grafted with PHEMA and not with PHEMA patterns.

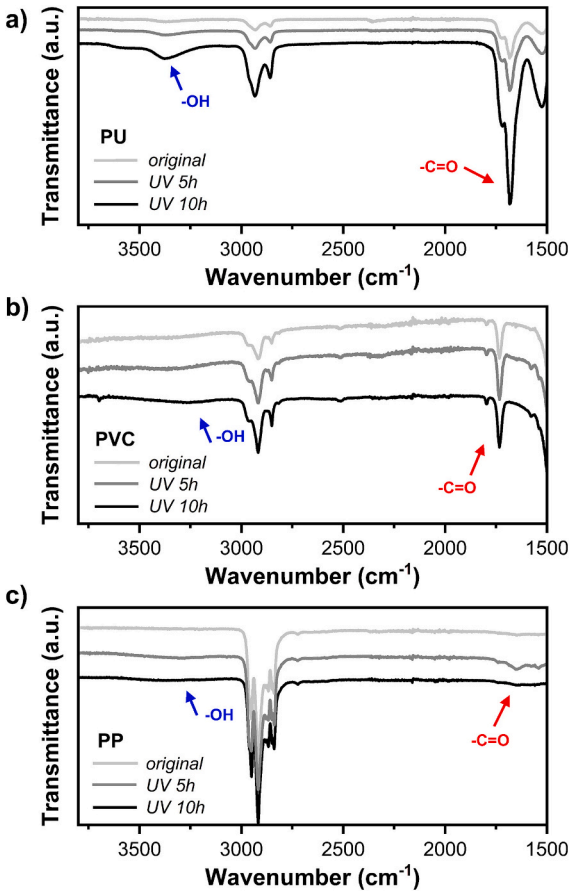


Fig. 5. FTIR spectra of a) PU, b) PVC, and c) PP substrates before and after UV exposure. For PU and PVC, the progressive increase in the intensity of bands associated with hydroxyl (–OH) stretching and carbonyl (C=O) vibrations with increasing UV exposure time indicates the formation of oxidized, hydrophilic surface functionalities. In contrast, PP exhibits an increase in –OH and C=O-related bands after 5 h of UV exposure, followed by a decrease after 10 h, consistent with UV-induced surface oxidation followed by hydrophobic recovery upon prolonged UV exposure.

where the planarization effect was more pronounced.

In contrast, PP exhibited a distinctly different response to UV exposure. While a small reduction in ice adhesion was observed after 5 h of UV irradiation (from 171 kPa to 164 kPa), prolonged exposure for 10 h resulted in a pronounced decrease in ice adhesion down to 85 kPa. The small decrease in ice adhesion after 5 h UV exposure is in contrast with the related contact angle decrease (Fig. 4a). The further decrease in ice adhesion is nevertheless well in agreement with the contact angle recovery observed after 10 h UV exposure with no surface roughness variations (Fig. 4a). This finding is particularly notable, as it suggests that prolonged UV exposure—typically associated with material degradation—may inadvertently decrease ice adhesion to PP substrates.

3.4. Role of oil and water lubrication in reducing ice adhesion

Passive anti-icing strategies based on interfacial lubrication are among the most effective approaches reported for reducing ice adhesion. These strategies generally rely on the presence of a lubricating layer between the ice and the solid surface, either in the form of a thin oil film [26] (LIS or SLIPS) or an unfrozen aqueous layer [35] (hydrated surfaces and hydrogels). In this work, both lubrication mechanisms were investigated: silicone oil microdroplets were used to represent partial oil lubrication, whereas hydrophilic coatings and grafted polymers were employed to promote the formation of interfacial water layers.

As shown in Fig. 6, contamination with silicone oil droplets reduced ice adhesion to all substrates compared to the unmodified surfaces. Ice adhesion decreased from 824 to 698 kPa on PU, from 687 to 582 kPa on PVC, and from 171 to 147 kPa on PP. This reduction follows the same qualitative trend reported for liquid-infused surfaces (LIS) [26], where the presence of a lubricating oil layer lowers the interfacial shear strength between ice and the substrate. However, in contrast to classical LIS systems, which typically reduce ice adhesion by one to two orders of magnitude, the reductions observed here are comparatively modest. This difference can be attributed to the absence of a continuous lubricant film: the present samples contain only discrete oil droplets. As a result, ice detachment occurred across regions of mixed contact between ice, oil, and the solid substrate, leading to a more limited and substrate-dependent reduction in ice adhesion. Notably, PP exposed to 10 h of UV irradiation exhibited a lower ice adhesion strength (85 kPa) than oil-covered PP (147 kPa), indicating that surface chemistry changes may, in some cases, outperform partial oil lubrication.

In contrast, surfaces with PHEMA (patterned or continuous hydrophilic surface treatment) exhibited a much stronger reduction in ice adhesion across all substrates. Ice adhesion decreased to 119 kPa on PU, 71 kPa on PVC, and 25 kPa on PP when patterned, and down to under 5 kPa (limit of our load cell) when the surfaces were fully covered with PHEMA. This behaviour is consistent with numerous reports demonstrating that hydrophilic polymer grafts can reduce ice adhesion through the formation of a lubricating aqueous layer at subzero temperatures. [15] Importantly, direct evidence for such a layer in the present system

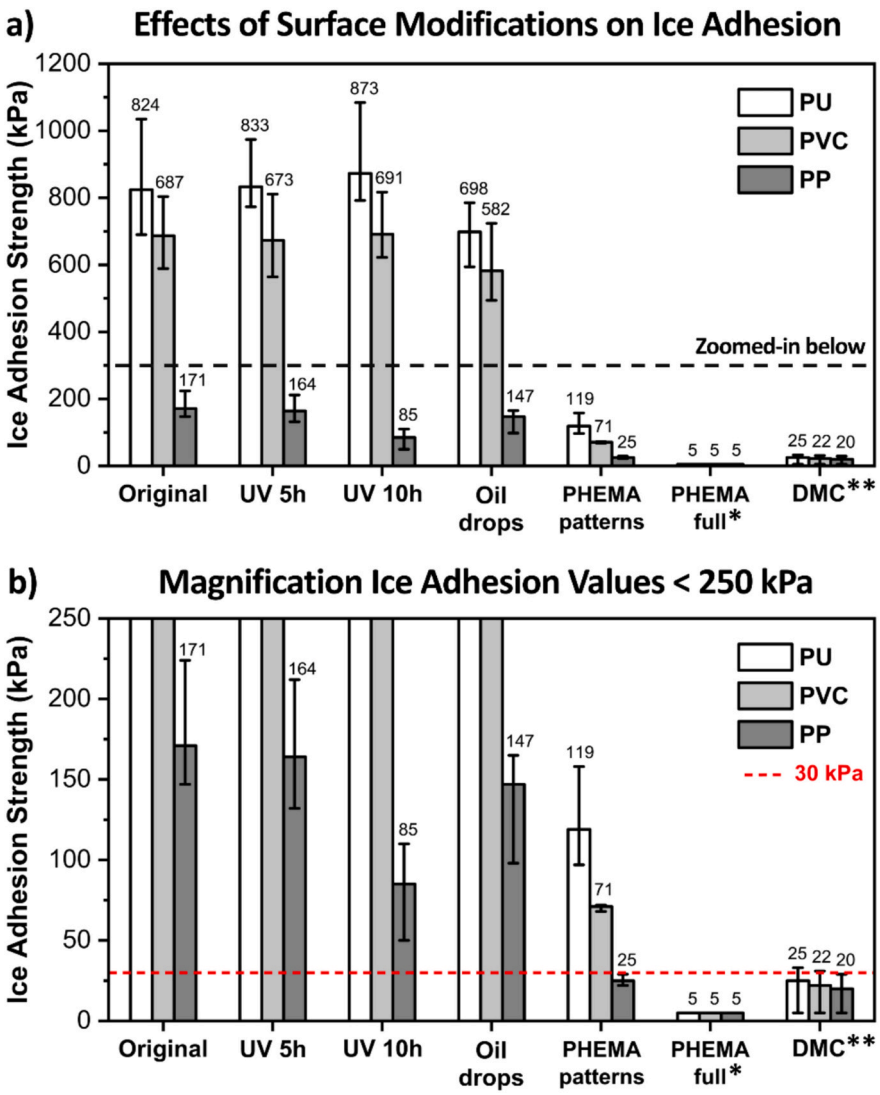


Fig. 6. Ice adhesion strength of PU, PVC, and PP substrates at −10 ± 1 °C and 5 ± 3% RH before and after surface modifications. a) Full range of measured ice adhesion values. b) Magnified view highlighting adhesion strengths below 250 kPa. The dashed red line indicates the commonly cited target value of 30 kPa for passive low-ice adhesion surfaces of use in aerospace. *Note 1:* For substrates fully grafted with PHEMA (*), the measured ice adhesion strengths were below the detection limit (5 kPa) in all experiments. *Note 2:* For DMC-coated samples (**), the measured ice adhesion strengths were below the detection limit (5 kPa) in some experiments, hence marking the lower limit. (For interpretation of the references to colour in this figure legend, the reader is referred to the web version of this article.)

was obtained in our previous work, where freezing events on identical PHEMA-patterned surfaces were shown to initiate on the hydrophilic regions to rapidly propagate along the stripes via a liquid-like molecular water layer (MWL). [39] Moreover, freezing on these regions was observed to occur only below approximately −15 °C, indicating that the interfacial water remains unfrozen at the ice adhesion testing temperature of −10 °C. These observations support the presence of a non-frozen interfacial water layer under the present conditions. Given the magnitude of the ice adhesion reduction, the grafted PHEMA patterns appear to generate a more effective lubricating interfacial layer than isolated hydrophobic silicone oil droplets or Teflon surfaces (Fig. 2).

To further examine the effect of surface coverage, fully PHEMA-grafted substrates were also prepared using the same procedure without a photomask. For these uniformly grafted samples, the measured ice adhesion strengths were below the detection limit of the experimental setup (~5 kPa) for all three polymer substrates. This observation supports the interpretation that a continuous hydrophilic layer can promote the formation of an interfacial water layer that enhances lubrication at the ice–substrate interface. In contrast, the patterned substrates offer only partial surface coverage, resulting in substrate-dependent adhesion values due to regions where ice remains in direct contact with the underlying polymer.

Surprisingly, no significant difference was observed between stripe orientations parallel and perpendicular to the pushing direction, despite the expectation that anisotropic surface features could influence local stress distributions and promote preferential crack initiation or propagation along specific directions. This indicates that the enhanced reduction in ice adhesion is governed primarily by improved interfacial lubrication associated with the patterned geometry, rather than by directional crack propagation or fracture mechanics under the tested conditions.

The formation of an unfrozen water layer at hydrophilic polymer interfaces is well documented for PHEMA and other hydrophilic polyacrylate-based materials. [36–38] Water-polymer chain interactions associated with such polymers are typically classified into three categories: freezable free water behaving similarly to bulk water, freezable bound water interacting weakly with the polymer chains, and non-freezing bound water strongly associated with hydrophilic or

charged functional groups. While freezable free water freezes near 0 °C, both freezable bound and non-freezing bound water can remain unfrozen well below typical freezing temperatures due to a balance between water–water hydrogen bonding, which promotes ice formation, and water–polymer interactions, which disrupt ice crystallization and stabilize liquid-like states.

Previous studies have shown that non-freezing water associated with PHEMA can remain in a liquid or quasi-liquid state down to approximately −15 °C. [37] At the testing temperature used in this work (−10 °C), both non-freezing and freezable bound water are therefore expected to remain unfrozen. Because the PHEMA grafts form a continuous hydrophilic phase within each patterned region, they can retain and stabilize interfacial water, leading to the formation of a lubricating layer. This liquid water layer reduces the effective ice–substrate contact area and lowers the shear stress required for ice detachment.

Among all strategies investigated in this work, the hydrophilic DMC coating produced the most pronounced reduction in ice adhesion. For all substrates, ice adhesion values fell below 30 kPa, reaching, in the worst, most extreme cases, 25 kPa on PU, 22 kPa on PVC, and 20 kPa on PP, with several samples showing ice adhesion below the detection limit of our device, i.e., below 5 kPa (Fig. 6). In all cases, these values are below the commonly cited threshold required for passive ice removal in aviation applications, where aerodynamic forces alone can promote dynamic ice shedding. As the DMC coating provides complete and continuous surface coverage, ice adhesion is governed by the coating surface chemistry itself rather than by the substrate beneath.

The particularly low ice adhesion values observed for all DMC-coated substrates are consistent with the formation of a water-lubricating layer at the ice-coating interface. In our previous work [40], thermal imaging experiments demonstrated the presence of a molecular water layer (MWL) on hydrophilic PHEMA-grafted surfaces, where freezing events rapidly propagated along the hydrated regions. While the presence of such a layer was not directly characterized for the DMC coating in the present study, previous investigations of hydrophilic methacrylate polymers have demonstrated the existence of non-freezing bound water associated with cationic quaternary ammonium groups at −10 °C using differential scanning calorimetry (DSC) and spectroscopic (FTIR) characterization. [52,53] The literature evidence, together with the exceptionally low adhesion values observed here, are therefore consistent with the presence of non-freezing bound-water inside the DMC-based polymer network, resulting in a replenishable aqueous lubricating layer similar to that formed on PHEMA-grafted surfaces.

Fig. 7 schematically summarizes the influence of each surface modification on the ice–substrate interface and the resulting ice adhesion behaviour and mechanism behind the ice adhesion. Despite being

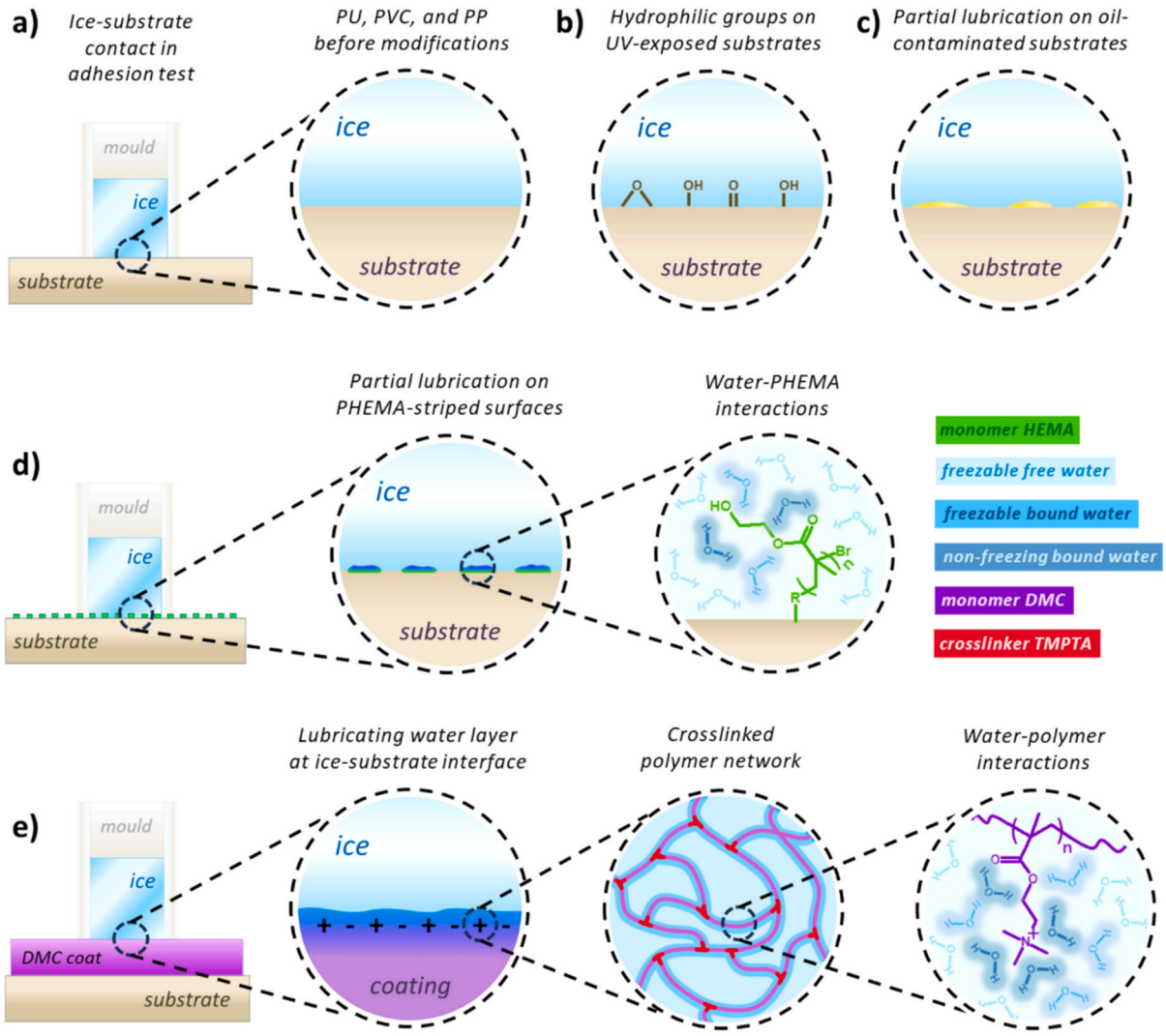


Fig. 7. Schematic overview of ice adhesion mechanisms for the investigated surface modifications. Ice–substrate interactions are shown for a) unmodified substrates, b) UV-exposed substrates covered with hydrophilic oxidation products, c) oil-contaminated surfaces with partial lubrication, d) PHEMA-patterned surfaces with partial aqueous lubricating layers, and e) DMC-coated surfaces covered with a continuous, replenishable water layer.

only slightly hydrophilic compared to PHEMA grafts, the greatest reduction in ice adhesion was achieved with the DMC coating and homogeneous PHEMA grafting, attributed to the formation of a continuous aqueous lubricating layer. In contrast to oil-based lubrication, which is inherently limited by lubricant depletion and leakage over time, water-based lubricating layers can be continuously replenished from the environment, making them a potentially more robust and sustainable strategy for long-term passive anti-icing applications. Moreover, the DMC coating of 50 μm thick is also expected to maintain icephobicity through the cross-section and possess higher durability than hydrophilic PHEMA brushes due to its crosslinked nature.

3.5. Comparison to existing anti-icing strategies and literature benchmarks

To place the results of this study in the context of previously reported low-ice-adhesion surfaces, Fig. 8 compares the ice adhesion strengths measured here with values from the literature [16,18,34,49,54–60,63–68,70–83,86–92] obtained under comparable conditions. Only studies employing horizontal shear-based ice adhesion tests at −10 ± 2 °C and reporting comparable ice geometries were included to ensure the fairest possible comparison (it should be noted that it was not possible to confirm the used RH in all studies due to a lack of available information).

As shown in Fig. 8a, hydrophobic (HS) and superhydrophobic surfaces (SHS) typically exhibit ice adhesion strengths in the range of ~100–500 kPa at −10 °C. Among these, a Teflon-based SHS [56] reported exceptionally low values below 30 kPa (≈10 kPa). Such performance is generally attributed to nanoscale surface structuring that minimizes effective ice–substrate contact via air entrapment and the hydrophobic nature of fluorocarbons. While this value is comparable to the one achieved by the DMC coating in the present work, nanostructured SHS are known to degrade rapidly under mechanical wear and repetitive icing–deicing cycles. [22–24] In addition, rising environmental concerns around the use of fluorinated materials question their suitability for aviation and other domains.

Elastic or soft polymer surfaces (ES) constitute another widely studied category for reducing ice adhesion, relying on elastic deformation during ice detachment. PDMS-based coatings, in particular, can achieve extremely low adhesion strengths (~3–10 kPa). However, these materials generally struggle with low mechanical robustness [25], making them unsuitable for demanding aeronautical environments despite their excellent laboratory performance.

Liquid-infused surfaces (LIS) are among the most recently extensively investigated passive anti-icing strategies and can consistently achieve low ice adhesion values in the range of ~5–100 kPa. As previously described for oil-contaminated samples, the effectiveness of LIS originates from the presence of a lubricating oil layer at the ice–surface interface. However, as with SHS and ES, their durability presents a key limitation. [28] The lubricating liquid is prone to depletion during repeated icing cycles, and, for that reason, maintaining a stable lubricant reservoir over time remains a significant challenge.

Water-lubricating surfaces (WLS) have recently emerged as an alternative strategy to overcome lubricant depletion by relying on a replenishable aqueous interfacial layer. As presented in Fig. 8a, WLS can achieve ice adhesion values comparable to or even lower than those of LIS. Nevertheless, many reported WLS rely on hydrogel-based materials that exhibit swelling and mechanical degradation under cyclic freezing conditions, limiting their applicability in aviation contexts.

Fig. 8b and c focus specifically on WLS and compare the performance of the PHEMA-patterned surfaces and DMC coating developed in this work with corresponding reported water-lubricating systems. Because material selection strongly influences durability and practical applicability, the reported studies were grouped into two categories: Fig. 8b compares the performance of PHEMA-grafted surfaces with other low-durability non-hard coating solutions, including hydrogels and surface grafts [34,64,65] with inherent mechanical limitations, and Fig. 8c compares the performance of the DMC coating with other coating systems, such as amphiphilic PEG-grafted coating formulations [63,66–68] that perform well in durability tests before icing tests but exhibit swelling or softening after repeated icing tests.

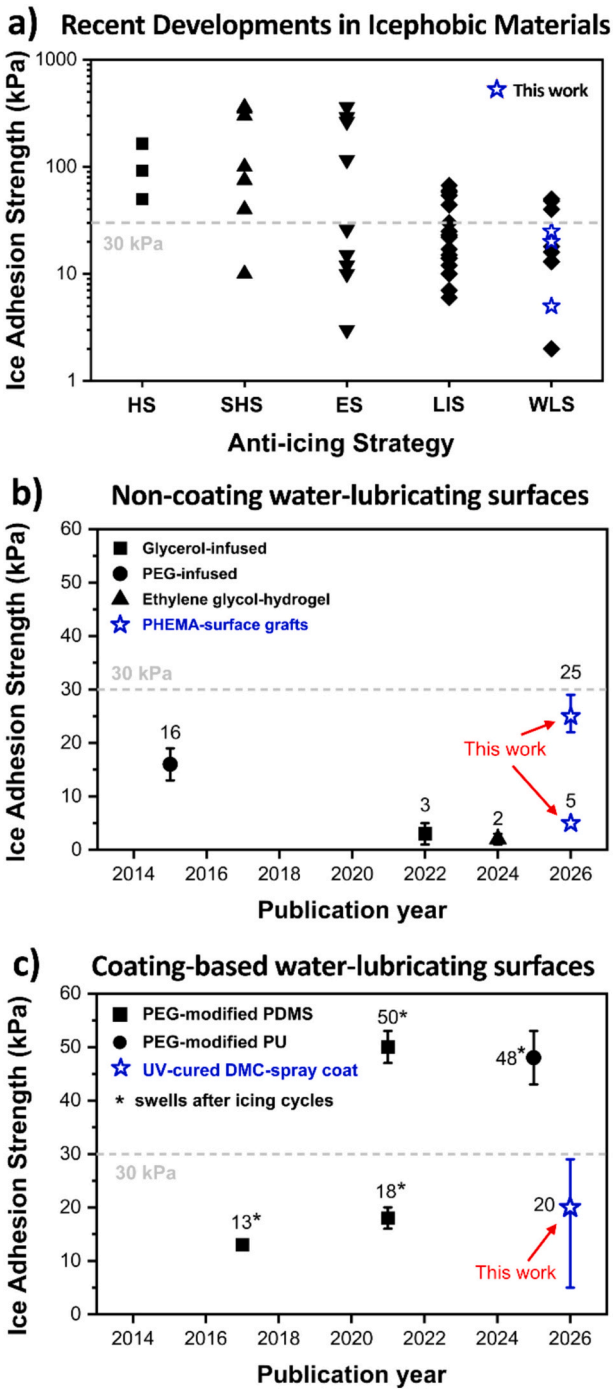


Fig. 8. Comparison of various passive low-ice adhesion strategies tested under comparable conditions using a horizontal shear test at −10 ± 2 °C. a) Ice adhesion [16,18,34,49,54–60,63–68,70–83,86–92] grouped by anti-icing strategy: hydrophobic (HS), superhydrophobic (SHS), elastic/soft polymers (ES), liquid-infused surfaces (LIS), and water-lubricating surfaces (WLS). b) Comparison of the ice adhesion performance of non-coating WLS as a function of publication year. c) Comparison of the ice adhesion performance of coating-based WLS as a function of publication year. The dashed lines at 30 kPa indicate a commonly cited threshold for sufficiently low ice adhesion.

The PHEMA-grafted surfaces investigated here fall within the lowest

range of reported ice adhesion values for hydrophilic non-hard coatings, particularly when included as full homogeneous coverage or patterns on PP. However, despite their strong anti-icing performance, such surface-initiated grafts have poor resistance to abrasion and erosion and therefore belong to the low-durability category.

In contrast, the PFAS-free DMC-based coating ranks among the lowest reported ice adhesion values, achieving adhesion strengths of max 20 kPa (with the lowest values below 5 kPa). These values are comparable to the best-performing water-lubricating systems reported in the literature, while offering substantially higher potential for durability and scalability. Notably, the DMC coating showed no visible degradation, delamination, or water absorption after 15 consecutive ice adhesion cycles, indicating encouraging mechanical stability even at this proof-of-concept stage. To further demonstrate the longevity of the DMC spray coating, Fig. 9 shows the evolution of the ice adhesion strength of the DMC-coated PP substrate monitored throughout the cyclic testing. The measured adhesion values remained consistently below 30 kPa over all 15 cycles with no systematic increase in adhesion strength. This observation indicates that repeated freezing and ice detachment did not result in measurable deterioration of the coating performance within the investigated test scheme. While longer durability studies involving environmental aging, abrasion, thermal cycling, and extended icing exposure will be required for aerospace qualification, these preliminary results show encouraging stability under repeated icing conditions.

Overall, many previously reported low-ice-adhesion surfaces remain unsuitable for aviation due to fabrication complexity, limited durability, or incompatibility with existing coating systems. While the SI-ATRP-based PHEMA micropatterning employed here performs sufficiently well even on PP, it is impractical for large-scale application due to its multistep preparation methodology, which uses expensive, specialized reagents. By contrast, the DMC coating, which is easily applied via spray coating and UV curing, can be deposited directly onto existing certified PU topcoats, where it exhibits very low ice adhesion and shows no visible deterioration over repeated testing. Collectively, these attributes position the DMC coating as a promising candidate for the future development of passive low-ice adhesion coatings for aircraft and other engineering applications.

Beyond purely passive use, recent studies have also explored hybrid anti-icing systems that combine passive low-adhesion surfaces with active photothermal or electrothermal de-icing. [93,94] While the main focus of the present work is in the development of fully passive anti-icing coatings, the DMC coating could also facilitate a gradual transition toward energy-saving icing protection systems. Since the coating can be applied directly onto existing aerospace polyurethane topcoats while maintaining very low ice adhesion, it could potentially be combined with current heating-based or electromechanical systems to reduce the energy required for ice removal. Such an approach may offer practical short-term benefits by lowering power consumption without requiring major modifications to existing aircraft anti-icing infrastructure. Future work could therefore also investigate the incorporation of photothermal absorbers into DMC-based coatings to evaluate possible synergistic effects between interfacial water lubrication and localized heating.

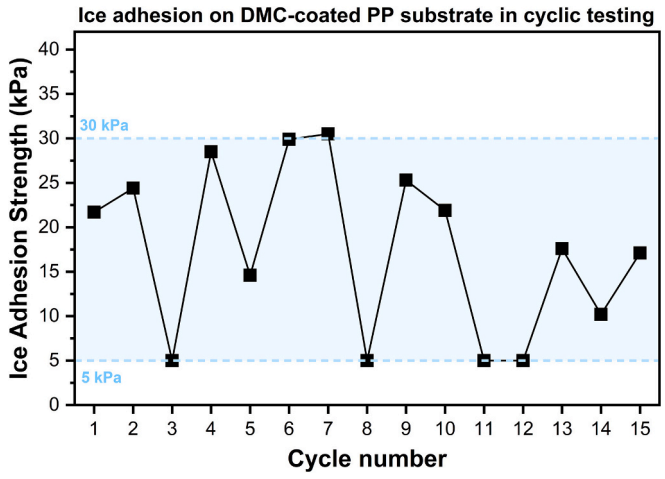


Fig. 9. Evolution of the ice adhesion strength on DMC-coated PP substrates at -10 ± 1 °C and 5 ± 3% RH during cyclic testing. The dashed blue lines indicate the commonly cited target value (30 kPa) for passive low-ice adhesion surfaces and the detection limit (5 kPa) of the ice adhesion test setup. (For interpretation of the references to colour in this figure legend, the reader is referred to the web version of this article.)

4. Conclusions

This work introduces a horizontal shear ice adhesion testing device with controlled environmental conditions and multiple sample holders, enabling reproducible measurements. Using this framework, the effects of five surface modifications on the ice adhesion behaviour of three polymer substrates (PVC, PP, and PU) were systematically investigated: short and prolonged UV exposure, silicone oil microdroplets, hydrophilic grafting with PHEMA, and a hydrophilic and cationic UV-curable DMC coating.

The results show that UV exposure induces a minor ice adhesion increase on PU and PVC due to the formation of hydrophilic oxidation products at the hard surface. In contrast, ice adhesion on PP decreases with UV exposure (10*h*) in a process of hydrophobic recovery. Silicone oil hydrophobic microdroplets consistently reduced ice adhesion, in agreement with previous studies on oil-infused passive anti-icing strategies. Notably, prolonged UV exposure proved more effective than oil contamination in reducing ice adhesion on PP.

Both hydrophilic surface modifications (PHEMA surface grafting and the 50 μm thick DMC coating) significantly reduced ice adhesion. This is attributed to the presence of non-freezing surface water later that can act as a lubricating layer at the ice–substrate interface. The more robust PFAS-free cationic DMC coating achieved low ice adhesion strengths of 20 kPa or lower (down to under 5 kPa), placing it among the lowest reported values for solid hydrophilic coatings tested under comparable testing conditions. Crucially, this performance is obtained using a simple UV-curable spray-coating process compatible with existing aviation-grade polyurethane coatings, showing no loss of ice adhesion under repeated testing, highlighting its potential for scalability and practical implementation.

Overall, this work provides a comparative framework for evaluating passive anti-icing strategies across different material classes and polymer substrates. It further demonstrates the potential of hydrophilic coatings as a promising foundation for the future development of durable, scalable, and aviation-compatible passive anti-icing treatments. Future work should focus on improving the coating chemistry, durability, and its behaviour in ice wind tunnels and high-speed supercooled droplet impact.

CRediT authorship contribution statement

M.J. Tavaststjerna: Writing – original draft, Visualization, Project administration, Methodology, Investigation, Data curation, Conceptualization. **R. Connolly:** Methodology, Data curation. **S. Caliari:** Investigation, Data curation. **S.J. Picken:** Writing – review & editing, Supervision, Conceptualization. **S.J. Garcia:** Writing – review & editing, Supervision, Project administration, Funding acquisition, Conceptualization.

Declaration of competing interest

The authors declare that they have no known competing financial interests or personal relationships that could have appeared to influence

the work reported in this paper.

Acknowledgments

This project has received funding from the European Union's Horizon 2020 research programme under the Marie Skłodowska-Curie grant agreement No 956703 (SURFICE project).

Appendix A. Supplementary data

Additional experimental and data analysis details, including photos of the samples and the ice adhesion test setup. Supplementary data to this article can be found online at doi:https://doi.org/10.1016/j.porgcoat.2026.110435.

Data availability

Data will be made available on request.

References

[1] O. Parent, A. Ilinca, Anti-icing and de-icing techniques for wind turbines: critical review, Cold Reg. Sci. Technol. 65 (2011) 88–96, https://doi.org/10.1016/j.coldregions.2010.01.005.
[2] K. Wei, Y. Yang, H. Zuo, D. Zhong, A review on ice detection technology and ice elimination technology for wind turbine, Wind Energy 23 (2020) 433–457, https://doi.org/10.1002/we.2427.
[3] L.H. De Koninck, S.F. Ahmadi, J.B. Boreyko, Passive anti-frosting cables, Int. J. Heat Mass Transf. 146 (2020) 118808, https://doi.org/10.1016/j.ijheatmasstransfer.2019.118808.
[4] J.L. Laforte, M.A. Allaire, J. Laflamme, State-of-the-art on power line de-icing, Atmos. Res. 46 (1998) 143–158, https://doi.org/10.1016/S0169-8095(97)00057-4.
[5] T. DiLorenzo, X. Yu, Use of ice detection sensors for improving winter road safety, Accid. Anal. Prev. 191 (2023) 107197, https://doi.org/10.1016/j.aap.2023.107197.
[6] A.P. Sarmiento, F.I.P. de Sá Sarmiento, A. Shooshtari, M. Ohadi, A review of recent progress in active frost prevention/control techniques in refrigeration and HVAC systems, Appl. Therm. Eng. 253 (2024) 123680, https://doi.org/10.1016/J.APPLTHERMALENG.2024.123680.
[7] Y. Cao, W. Tan, Z. Wu, Aircraft icing: an ongoing threat to aviation safety, Aerosp. Sci. Technol. 75 (2018) 353–385, https://doi.org/10.1016/j.ast.2017.12.028.
[8] M. Yamazaki, A. Jemcov, H. Sakaue, A review on the current status of icing physics and mitigation in aviation, Aerospace 8 (2021), https://doi.org/10.3390/aerospace8070188.
[9] K. Wang, Y. Xue, H. Tian, M. Wang, X. Wang, The impact of icing on the airfoil on the lift-drag characteristics and maneuverability characteristics, Math. Probl. Eng. 2021 (2021) 5568740, https://doi.org/10.1155/2021/5568740.
[10] Z. Wu, Drop "impact" on an airfoil surface, Adv. Colloid Interf. Sci. 256 (2018) 23–47, https://doi.org/10.1016/J.CIS.2018.05.005.
[11] F.T. Lynch, A. Khodadoust, Effects of ice accretions on aircraft aerodynamics, Prog. Aerosp. Sci. 37 (2001) 669–767, https://doi.org/10.1016/S0376-0421(01)00018-5.
[12] F. Caliskan, C. Hajiyev, A review of in-flight detection and identification of aircraft icing and reconfigurable control, Prog. Aerosp. Sci. 60 (2013) 12–34, https://doi.org/10.1016/J.PAEROSCI.2012.11.001.
[13] Q. HE, K. LI, Z. XU, J. WANG, X. WANG, A. LI, Research progress on construction strategy and technical evaluation of aircraft icing accretion protection system, Chin. J. Aeronaut. 36 (2023) 1–23, https://doi.org/10.1016/J.CJA.2023.07.003.
[14] R. Rekuviene, S. Saeidiharzand, L. Mažeika, V. Samaitis, A. Jankauskas, A. K. Sadaghiani, G. Gharib, Z. Muganlı, A. Koşar, A review on passive and active anti-icing and de-icing technologies, Appl. Therm. Eng. 250 (2024) 123474, https://doi.org/10.1016/J.APPLTHERMALENG.2024.123474.
[15] P. Irajizad, S. Nazifi, H. Ghasemi, Icephobic surfaces: definition and figures of merit, Adv. Colloid Interf. Sci. 269 (2019) 203–218, https://doi.org/10.1016/j.cis.2019.04.005.
[16] K. Golovin, S.P.R. Kobaku, D.H. Lee, E.T. DiLoreto, J.M. Mabry, A. Tuteja, Designing durable icephobic surfaces, Sci. Adv. 2 (2016), https://doi.org/10.1126/sciadv.1501496.
[17] Y. Zhan, Z. Pang, G. Tan, Advances in icephobic coatings: concepts, mechanisms, classifications and prospects, Cold Reg. Sci. Technol. 239 (2025) 104596, https://doi.org/10.1016/J.COLDREGIONS.2025.104596.
[18] J. Chen, R. Dou, D. Cui, Q. Zhang, Y. Zhang, F. Xu, X. Zhou, J. Wang, Y. Song, L. Jiang, Robust prototypical anti-icing coatings with a self-lubricating liquid water layer between ice and substrate, ACS Appl. Mater. Interfaces 5 (2013) 4026–4030, https://doi.org/10.1021/am401004t.
[19] R. Dou, J. Chen, Y. Zhang, X. Wang, D. Cui, Y. Song, L. Jiang, J. Wang, Anti-icing coating with an aqueous lubricating layer, ACS Appl. Mater. Interfaces 6 (2014) 6998–7003, https://doi.org/10.1021/am501252u.
[20] Z. He, Y. Zhuo, Z. Zhang, J. He, Design of Icephobic Surfaces by lowering ice adhesion strength: a Mini review, Coatings 11 (2021), https://doi.org/10.3390/coatings11111343.
[21] M. Ferrari, F. Cirisano, Superhydrophobic coating solutions for deicing control in aircraft, Appl. Sci. 13 (2023), https://doi.org/10.3390/app132111684.
[22] S.A. Kulinich, S. Farhadi, K. Nose, X.W. Du, Superhydrophobic surfaces: are they really ice-repellent? Langmuir 27 (2011) 25–29, https://doi.org/10.1021/la104277q.
[23] S. Jung, M. Dorrestijn, D. Raps, A. Das, C.M. Megaridis, D. Poulikakos, Are superhydrophobic surfaces best for icephobicity? Langmuir 27 (2011) 3059–3066, https://doi.org/10.1021/la104762g.
[24] J. Chen, J. Liu, M. He, K. Li, D. Cui, Q. Zhang, X. Zeng, Y. Zhang, J. Wang, Y. Song, Superhydrophobic surfaces cannot reduce ice adhesion, Appl. Phys. Lett. 101 (2012), https://doi.org/10.1063/1.4752436.
[25] Y. Zhuo, S. Xiao, A. Amirfazli, J. He, Z. Zhang, Polysiloxane as icephobic materials – the past, present and the future, Chem. Eng. J. 405 (2021) 127088, https://doi.org/10.1016/J.CEJ.2020.127088.
[26] S. Heydarian, R. Jafari, G. Momen, Recent progress in the anti-icing performance of slippery liquid-infused surfaces, Prog. Org. Coat. 151 (2021) 106096, https://doi.org/10.1016/J.PORGCOAT.2020.106096.
[27] M. Villegas, Y. Zhang, N. Abu Jarad, L. Soleymani, T.F. Didar, Liquid-infused surfaces: a review of theory, design, and applications, ACS Nano 13 (2019) 8517–8536, https://doi.org/10.1021/acsnano.9b04129.
[28] S. Peppou-Chapman, J.K. Hong, A. Waterhouse, C. Neto, Life and death of liquid-infused surfaces: a review on the choice, analysis and fate of the infused liquid layer, Chem. Soc. Rev. 49 (2020) 3688–3715, https://doi.org/10.1039/d0cs00036a.
[29] M. Shamshiri, R. Jafari, G. Momen, A novel hybrid anti-icing surface combining an aqueous self-lubricating coating and phase-change materials, Prog. Org. Coat. 177 (2023) 107414, https://doi.org/10.1016/j.porgcoat.2023.107414.
[30] M. Shamshiri, G. Momen, R. Jafari, Icephobic coatings beyond boundaries: layered integration of phase change materials beneath a PEG-PDMS copolymer–containing coating to enhance anti-icing performance, Prog. Org. Coat. 189 (2024) 108324, https://doi.org/10.1016/J.PORGCOAT.2024.108324.
[32] Z. He, Y. Zhuo, F. Wang, J. He, Z. Zhang, Design and preparation of icephobic PDMS-based coatings by introducing an aqueous lubricating layer and macro-crack initiators at the ice-substrate interface, Prog. Org. Coat. 147 (2020) 105737, https://doi.org/10.1016/j.porgcoat.2020.105737.
[33] R.A. Biro, E. Thormann, Ice adhesion to cationic, anionic, Zwitterionic, and nonionic polymer surfaces, ACS Appl. Polym. Mater. 6 (2024) 13744–13752, https://doi.org/10.1021/acsapm.4c02572.
[34] S. Ozbay, C. Yuceel, H.Y. Erbil, Improved Icephobic properties on surfaces with a hydrophilic lubricating liquid, ACS Appl. Mater. Interfaces 7 (2015) 22067–22077, https://doi.org/10.1021/acsami.5b07265.
[35] J. Chen, Z. Luo, Q. Fan, J. Lv, J. Wang, Anti-ice coating inspired by ice skating, Small 10 (2014) 4693–4699, https://doi.org/10.1002/smll.201401557.
[36] S. Abasi, R. Davis, D.A. Podstawczyk, A. Guiseppi-Elie, Distribution of water states within poly(HEMA-co-HPMA)-based hydrogels, Polymer (Guildf). 185 (2019) 121978, https://doi.org/10.1016/J.POLYMER.2019.121978.
[37] V.M. Gun'ko, I.N. Savina, S.V. Mikhalovsky, Properties of water bound in hydrogels, Gels 3 (2017), https://doi.org/10.3390/GELS3040037.
[38] L. Guan, H. Xu, D. Huang, The investigation on states of water in different hydrophilic polymers by DSC and FTIR, J. Polym. Res. 18 (2011) 681–689, https://doi.org/10.1007/S10965-010-9464-7.
[39] S. Rønneberg, J. He, Z. Zhang, The need for standards in low ice adhesion surface research: a critical review, J. Adhes. Sci. Technol. 34 (2020) 319–347, https://doi.org/10.1080/01694243.2019.1679523.
[40] M.J. Tavaststjerna, S.J. Picken, S.J. Garcia, Controlling frost propagation on polymeric surfaces using SI-ATRP chemical micropatterning, Adv. Mater. Interfaces 12 (2025) 2400838, https://doi.org/10.1002/admi.202400838.
[41] M.J. Tavaststjerna, M. Ding, J. Hussong, S.J. Picken, I.V. Roisman, S.J. Garcia, The influence of chemical surface patterning on the freezing behaviour of impacting supercooled water droplets, Surf. Interfaces 76 (2025) 107918, https://doi.org/10.1016/J.SURFIN.2025.107918.
[42] L. Stendardo, G. Gastaldo, M. Budinger, V. Pommier-Budinger, I. Tagliaro, P. F. Ibáñez-Ibáñez, C. Antonini, Reframing ice adhesion mechanisms on a solid surface, Appl. Surf. Sci. 641 (2023) 158462, https://doi.org/10.1016/J.APSUSC.2023.158462.
[43] G. Hernández Rodríguez, M. Fratschko, L. Stendardo, C. Antonini, R. Resel, A. M. Coclite, Icephobic gradient polymer coatings deposited via iCVD: a novel approach for icing control and mitigation, ACS Appl. Mater. Interfaces 16 (2024) 11901–11913, https://doi.org/10.1021/acsami.3c18630.
[44] L. Stendardo, G. Gastaldo, M. Budinger, I. Tagliaro, V. Pommier-Budinger, C. Antonini, Why the adhesion strength is not enough to assess ice adhesion on surfaces, Appl. Surf. Sci. 672 (2024) 160740, https://doi.org/10.1016/J.APSUSC.2024.160740.
[45] K. Golovin, A. Dhyani, M.D. Thouless, A. Tuteja, Low–interfacial toughness materials for effective large-scale deicing, Science 364 (2019) (1979) 371–375, https://doi.org/10.1126/science.aav1266.
[46] C. (Chris) Qin, A.T. Mulroney, M.C. Gupta, Anti-icing epoxy resin surface modified by spray coating of PTFE Teflon particles for wind turbine blades, Mater. Today Commun. 22 (2020) 100770, https://doi.org/10.1016/J.MTCOMM.2019.100770.
[47] R. Haehnel, Evaluation of coatings for icing control at hydraulic structures, Ice Eng. 33 (January 2002) 5, 2002.

[48] M. Landy, A. Freiberger, Studies of ice adhesion: I. Adhesion of ice to plastics, J. Colloid Interface Sci. 25 (1967) 231–244, https://doi.org/10.1016/0021-9797(67)90026-4.
[49] A.J. Meuler, J.D. Smith, K.K. Varanasi, J.M. Mabry, G.H. McKinley, R.E. Cohen, Relationships between water wettability and ice adhesion, ACS Appl. Mater. Interfaces 2 (2010) 3100–3110, https://doi.org/10.1021/am1006035.
[50] T. Lu, E. Solis-Ramos, Y. Yi, M. Kumosa, UV degradation model for polymers and polymer matrix composites, Polym. Degrad. Stab. 154 (2018) 203–210, https://doi.org/10.1016/J.POLYMDEGRADSTAB. 2018.06.004.
[51] G. Primc, Hydrophilization of polypropylene by gaseous plasma treatments and hydrophobic recovery, Polymers (Basel). 17 (2025), https://doi.org/10.3390/polym17192644.
[52] I.E. Sørensen, E. Thormann, Freezing point depression of aqueous polyelectrolyte solutions: effects of chain length, charge density, and Counterion type, Macromolecules 59 (2026) 6500–6508, https://doi.org/10.1021/acs.macromol.6c00180.
[53] S. Chernyy, M. Järn, K. Shimizu, A. Swerin, S.U. Pedersen, K. Daasbjerg, L. Makkonen, P. Claesson, J. Iruthayaraj, Superhydrophilic polyelectrolyte brush layers with imparted anti-icing properties: effect of counter ions, ACS Appl. Mater. Interfaces 6 (2014) 6487–6496, https://doi.org/10.1021/am500046d.
[54] L. Liu, S. Chen, Y. Hu, W. Pan, T. Dong, Y. Chen, L. Lin, L. Wang, Anti-/deicing membranes with damage detection and fast healing, Adv. Funct. Mater. 34 (2024) 2404760, https://doi.org/10.1002/adfm.202404760.
[55] Q. Yang, Z. Zhu, S. Tan, Y. Luo, Z. Luo, How Micro-/nanostructure evolution influences dynamic wetting and natural deicing abilities of bionic Lotus surfaces, Langmuir 36 (2020) 4005–4014, https://doi.org/10.1021/acs.langmuir.0c00145.
[56] E. Vazirinasab, K. Maghsoudi, R. Jafari, G. Momen, A comparative study of the icephobic and self-cleaning properties of Teflon materials having different surface morphologies, J. Mater. Process. Technol. 276 (2020) 116415, https://doi.org/10.1016/J.JMATPROTEC.2019.116415.
[57] Y. Liu, Z. Zhang, H. Hu, H. Hu, A. Samanta, Q. Wang, H. Ding, An experimental study to characterize a surface treated with a novel laser surface texturing technique: water repellency and reduced ice adhesion, Surf. Coat. Technol. 374 (2019) 634–644, https://doi.org/10.1016/J.SURFCOAT.2019.06.046.
[58] N. Wang, L. Tang, W. Tong, D. Xiong, Fabrication of robust and scalable superhydrophobic surfaces and investigation of their anti-icing properties, Mater. Des. 156 (2018) 320–328, https://doi.org/10.1016/J.MATDES.2018.06.053.
[59] Q. Fu, X. Wu, D. Kumar, J.W.C. Ho, P.D. Kanhere, N. Srikanth, E. Liu, P. Wilson, Z. Chen, Development of sol–gel icephobic coatings: effect of surface roughness and surface energy, ACS Appl. Mater. Interfaces 6 (2014) 20685–20692, https://doi.org/10.1021/am504348x.
[60] W. Cui, T.A. Pakkanen, Fabrication of transparent icephobic surfaces with self-reparability: effect of structuring and thickness of the lubricant-elastomer layer, Appl. Surf. Sci. 504 (2020) 144061, https://doi.org/10.1016/J.APSUSC.2019.144061.
[63] M. Bakhtiari, E. Bakhshandeh, R. Jafari, G. Momen, Enhancing anti-icing efficacy in hybrid polyurethane coatings: evaluating the significance of molecular weight, chemical structure, and content of PEG/PDMS, Appl. Surf. Sci. 684 (2025) 161951, https://doi.org/10.1016/J.APSUSC.2024.161951.
[64] Y. Zhang, W. Yan, Y. Lin, J. Zhu, H. Zhao, T. Li, Multifunctional anti-icing gel surface with enhanced durability, ACS Appl. Mater. Interfaces 16 (2024) 14198–14207, https://doi.org/10.1021/acsami.4c00617.
[65] A. Ijaz, A. Miko, A.L. Demirel, Low ice adhesion anti-icing coatings based on PEG release from mesoporous silica particle loaded SBS, Mater. Adv. 3 (2022) 8168–8177, https://doi.org/10.1039/D2MA00661H.
[66] M. Shamshiri, R. Jafari, G. Momen, Icephobic properties of aqueous self-lubricating coatings containing PEG-PDMS copolymers, Prog. Org. Coat. 161 (2021) 106466, https://doi.org/10.1016/J.PORGCOAT.2021.106466.
[67] A. Rahimi, M. Murphy, V. Upadhyay, K. Faiyaz, D. Battocchi, D.C. Webster, Amphiphilically modified self-stratified siloxane-glycidyl carbamate coatings for anti-icing applications, J. Coat. Technol. Res. 18 (2021) 83–97, https://doi.org/10.1007/s11998-020-00402-8.
[68] V. Upadhyay, T. Galhenage, D. Battocchi, D. Webster, Amphiphilic icephobic coatings, Prog. Org. Coat. 112 (2017) 191–199, https://doi.org/10.1016/J.PORGCOAT.2017.07.019.
[70] S.G. Moghadam, E. Bakhshandeh, R. Jafari, G. Momen, In-depth analysis of the effect of physicochemical properties of ionic liquids on anti-icing behavior of silicon based-coatings, Cold Reg. Sci. Technol. 216 (2023) 104007, https://doi.org/10.1016/J.COLDREGIONS.2023.104007.
[71] X. Wang, Z. Lin, A novel high-performance coating with hybrid nanofiller reinforcement for superior self-cleaning, anti-icing, and corrosion resistance properties, J. Build. Eng. 80 (2023) 107993, https://doi.org/10.1016/J.JOBE.2023.107993.
[72] J.V. Buddingh, G. Liu, Hard epoxy coating with lasting low ice adhesion strength, ACS Appl. Polym. Mater. 5 (2023) 7485–7496, https://doi.org/10.1021/acsapm.3c01360.
[73] S. Heydarian, G. Momen, R. Jafari, Icephobicity and electrical assessment of slippery coating impregnated with a stabilized hydroxyl-terminated lubricant for high voltage insulation application, J. Mater. Sci. 58 (2023) 9264–9281, https://doi.org/10.1007/s10853-023-08600-6.
[74] Y. Liu, S. Gao, J. Liu, Q. Zhang, Biomimetic slippery liquid-infused porous surfaces fabricated by porous fluorinated polyurethane films for anti-icing property, Prog. Org. Coat. 179 (2023) 107524, https://doi.org/10.1016/J.PORGCOAT.2023.107524.
[75] B. Becher-Nienhaus, G. Liu, J.V. Buddingh, H. Zheng, Robust polyurethane coatings with lightly cross-linked surfaces for ice shedding, ACS Appl. Polym. Mater. 5 (2023) 3119–3128, https://doi.org/10.1021/acsapm.3c00259.
[76] H. Qi, X. Lei, J. Gu, Y. Zhang, X. Gu, G. Zhao, J. Yu, Low modulus of polydimethylsiloxane organogel coatings induced low ice adhesion, Prog. Org. Coat. 177 (2023) 107435, https://doi.org/10.1016/J.PORGCOAT.2023.107435.
[77] S.J. Lee, G. Do Park, Effective icephobicity of silicone oil-infused oleamide–polydimethylsiloxane with enhanced lubrication lifetime, ACS Omega 7 (2022) 21156–21162, https://doi.org/10.1021/acsomega.2c01956.
[78] J. Yuan, Y. Huang, H. Li, L. Jiang, Y. Dan, Preparation and anti-icing performance of cross-linked polysiloxane coatings containing silicone oil, React. Funct. Polym. 170 (2022) 105124, https://doi.org/10.1016/J.REACTFUNCTPOLYM.2021.105124.
[79] Y. Tian, Y. Liu, Z. Su, S. Wang, B. Zhang, H. Zhang, Q. Zhang, Biomimetic Brushlike slippery coatings with mechanically robust, self-cleaning, and Icephobic properties, ACS Appl. Mater. Interfaces 12 (2020) 54041–54052, https://doi.org/10.1021/acsami.0c14042.
[80] Y. Liu, Y. Tian, J. Chen, H. Gu, J. Liu, R. Wang, B. Zhang, H. Zhang, Q. Zhang, Design and preparation of bioinspired slippery liquid-infused porous surfaces with anti-icing performance via delayed phase inversion process, Colloids Surf. A Physicochem. Eng. Asp. 588 (2020) 124384, https://doi.org/10.1016/J.COLSURFA.2019.124384.
[81] S. Barthwal, B. Lee, S.H. Lim, Fabrication of robust and durable slippery anti-icing coating on textured superhydrophobic aluminum surfaces with infused silicone oil, Appl. Surf. Sci. 496 (2019) 143677, https://doi.org/10.1016/J.APSUSC.2019.143677.
[82] T. Yamazaki, M. Tenjimbayashi, K. Manabe, T. Moriya, H. Nakamura, T. Nakamura, T. Matsubayashi, Y. Tsuge, S. Shiratori, Antifreeze liquid-infused surface with high transparency, low ice adhesion strength, and Antifrosting properties fabricated through a spray layer-by-layer method, Ind. Eng. Chem. Res. 58 (2019) 2225–2234, https://doi.org/10.1021/acs.iecr.8b05927.
[83] A. Sandhu, O.J. Walker, A. Nistal, K.L. Choy, A.J. Clancy, Perfluoroalkane wax infused gels for effective, regenerating, anti-icing surfaces, Chem. Commun. 55 (2019) 3215–3218, https://doi.org/10.1039/C8CC09818B.
[86] P. Li, J. Yuan, L. Lan, Y. Dan, L. Jiang, Y. Huang, Durable and organic-solvent-free anti-icing coating fabricated from polyacrylate grafted with PDMS, Polymer (Guildf). 317 (2025) 127857, https://doi.org/10.1016/J.POLYMER.2024.127857.
[87] T. Zhu, Y. Yuan, L. Song, X. Wei, H. Xiang, X. Dai, X. Hua, R. Liao, A PDMS coating with excellent durability for large-scale deicing, J. Mater. Res. Technol. 29 (2024) 4526–4536, https://doi.org/10.1016/J.JMRT.2024.02.177.
[88] A.A.S. Adja, S. Sobhani, G. Momen, I. Fofana, J. Carrière, Step by step progress to achieve an icephobic silicone-epoxy hybrid coating: tailoring matrix composition and additives, J. Appl. Polym. Sci. 140 (2023) e54262, https://doi.org/10.1002/app.54262.
[89] M. Shamshiri, R. Jafari, G. Momen, An intelligent icephobic coating based on encapsulated phase change materials (PCM), Colloids Surf. A Physicochem. Eng. Asp. 655 (2022) 130157, https://doi.org/10.1016/J.COLSURFA.2022.130157.
[90] J. Sarma, L. Zhang, Z. Guo, X. Dai, Sustainable icephobicity on durable quasi-liquid surface, Chem. Eng. J. 431 (2022) 133475, https://doi.org/10.1016/J.CEJ.2021.133475.
[91] H. Teisala, P. Baumli, S.A.L. Weber, D. Vollmer, H.-J. Butt, Grafting silicone at room temperature—a transparent, scratch-resistant nonstick molecular coating, Langmuir 36 (2020) 4416–4431, https://doi.org/10.1021/acs.langmuir.9b03223.
[92] M. Bleszynski, R. Woll, J. Middleton, M. Kumosa, Effects of crosslinking, embedded TiO2 particles and extreme aging on PDMS icephobic barriers, Polym. Degrad. Stab. 166 (2019) 272–282, https://doi.org/10.1016/J.POLYMDEGRADSTAB.2019.06.005.
[93] Z. He, H. Xie, M.I. Jamil, T. Li, Q. Zhang, Electro-/photo-thermal promoted anti-icing materials: a new strategy combined with passive anti-icing and active de-icing, Adv. Mater. Interfaces 9 (2022) 2200275, https://doi.org/10.1002/admi.202200275.
[94] G. Gastaldo, G. Hernández-Rodríguez, V. Pommier-Budinger, M. Budinger, J. Pothin, A.M. Coclite, Impact of coatings on the performance of resonant electromechanical de-icing systems, Results Eng. 27 (2025) 106636, https://doi.org/10.1016/j.rineng.2025.106636.